Correlation-Based Contraction Tracking of Cardiomyocyte Monolayers

Samuel Frankel

A thesis

submitted in partial fulfillment of the

requirements for the degree of

Master of Science in Bioengineering

University of Washington

2014

Committee:

Deok-Ho Kim

Michael Regnier

Jinkyu Yang

Program Authorized to Offer Degree:

College of Engineering

University of Washington

Abstract

Correlation-Based Contraction Tracking of Cardiomyocyte Monolayers

Samuel Frankel

Chair of the Supervisory Committee:

Dr. Deok-Ho Kim

Bioengineering

Cardiac tissue engineering has made great strides in combating cardiovascular disease in modern society utilizing cardiac regenerative medicine as well as *in vitro* disease modeling. Stem cell-derived cardiomyocytes are a promising path to tissue regeneration, but the technology is not fully developed, as fully functional cardiac tissue phenotypically similar to the native tissue in humans has not yet been created. Many engineered cardiac tissues lack the orientation of highly aligned native cardiac tissue, and lack the mature sarcomeric structures that adult human cardiomyocytes have. Therefore, quantification of cardiomyocyte function and maturity is of critical importance in order to measure the effectiveness of these engineered tissues in mimicking the phenotype of native cardiac tissues. Specifically, the quality of contractile motion is very important, as it is a direct indicator of the status of the structural maturity of the sarcomeres—the organized contractile motor units. Past research has implemented a variety of methods to track and quantify cardiomyocyte contractions, but many of them share limitations

derived from either the methodological parameters or from the available resultant physiologically relevant endpoints.

In this thesis we present an application of entirely optical contraction analysis that expands upon previous applications. Using this MATLAB and C++-based software utilizing Particle Image Velocimetry (PIV) and Digital Image Correlation (DIC) algorithms, a variety of physiologically relevant contractile endpoints can be determined from brightfield video data of engineered cardiomyocyte tissues. We will validate the accuracy of this method Using micropost arrays as well as nanopatterned substrates in conjunction with primary cardiomyocytes, human embryonic stem cell-derived cardiomyocytes, and human induced pluripotent stem cell-derived cardiomyocytes. We will then apply these algorithms, referred to as Correlation-based Contraction Quantification (CCQ) to a case study to analyze the behavior of Duchenne Muscular Dystrophy, a genetic cardiomyopathy, in *in vitro* tissues to illustrate the benefit of such software in applications to disease models.

Acknowledgements

I would like to extend my deep and sincere gratitude to Dr. Deok-Ho Kim, my advisor as both an undergraduate and graduate student. Dr. Kim is extremely passionate about his research, and his enthusiasm is both obvious and infectious. Dr. Kim has always pushed me to create the highest quality research, and to hold myself to the highest standards of my work. Under his guidance, I have learned to take a great deal of pride in the research that I do. I greatly appreciate the opportunity he has given me to do research in his laboratory.

I would also like to thank Dr. Jinkyu Yang, a member of my thesis committee and faculty in the department of Aeronautics and Astronautics Engineering. I was able to collaborate with Dr. Yang's laboratory and work closely with a graduate student in the lab, Ehsan Nasr Esfahani. Dr. Yang is an encouraging and kind PI, and Ehsan provided me with valuable assistance in learning and executing valuable code for my project. I would also like to thank Dr. Mike Regnier for the assistance and time he offered as a committee member for my thesis.

Jesse Macadangdang, a PhD student in the Kim lab, provided me with valuable guidance as my direct mentor in Dr. Kim's lab through both my undergraduate and graduate studies. He consistently provided support and fresh perspective to the challenges I faced, and I consider him one of the most capable scientists I have had the pleasure of working with. Kshitiz, a previous postdoc in the Kim laboratory, always could provide valuable insight and motivation, and he played a large role in my understanding of how the field of academic research functions. He is clearly a scientist due to his love of exploring the unknown, and this aspect of his person has made a deep impression upon me. Alex Jiao and Peter Kim are two PhD candidates who have helped me greatly in the Kim lab, providing valuable data for my project, as well as personal support. Paulos Mengstaub, a post-baccalaureate in the Kim lab, was always eager to help, and

the two of us spent many hours during sleepless nights troubleshooting and implementing various computational analysis methods. Finally, Jinsung Kim, an undergraduate and one of the hardest workers in the Kim lab, did his best to always come through for those who counted on him for imaging and other laboratory processes. Thank you to each member of the Kim lab for their support, both direct and indirect, during this process.

Finally, I would like to thank my family and friends for supporting me throughout my education and life. My parents, Art and Pia, have always believed in me and supported my goals no matter the direction I took them. They have impressed upon me the importance of a strong work ethic, and I would not be where I am today without their influence. My sister Sarah is always encouraging and continually optimistic in the face of all manner of challenges. My family and friends, including those I have omitted here, have given me a great impetus to succeed in my academic and personal goals.

Table of Contents

List of Figures

CHAPTER 1: INTRODUCTION

1.1 *Motivation*

Cardiac tissue engineering primarily aims to design cardiac tissue that accurately mimics the behavior of the native heart. The behavior of the heart is characterized by the ability to mechanically move blood throughout the human body based on synchronized physical contraction at a cellular level. Creating *in vitro* engineered tissue with phenotypic similarities to adult human cardiomyocyte tissue brings relevancy to three primary applications of cardiac tissue engineering, direct therapy, disease modeling, and drug screening. Previously direct therapy, disease modeling, and drug screening have often been studied via single cell adult cardiomyocyte studies. However, limitations are present in single cell studies due to a dichotomy between the behaviors of cells in single-cell environments compared to confluent tissue environments. Differences in this behavior make it difficult to draw accurate comparisons between results of single-cell studies and the predicted behavior of cardiac tissue in an adult human.

To overcome the physiological differences between single cell and tissue-level behaviors, many studies currently use cardiomyocyte tissue systems for analysis, which more accurately model the behavior of the systems of cells inside the adult human body. These tissues often are derived from primary rat cardiomyocytes, which are commonly studied and easily available. However, these rat cardiomyocytes have different physiological behaviors compared to human cardiomyocytes. As such, current research explores the usage of differentiated human pluripotent stem cell-derived cardiomyocytes (hPSC-CMs). However, these differentiated tissues are often

not mature enough to share the phenotypic behaviors of adult cardiac tissue. Relevant metrics are necessary to determine the similarities or relationships in phenotype between *in vitro* cardiomyocyte tissues and adult human cardiac tissues, including electrophysiological analyses, structural analyses, and mechanical analyses.

Various methodologies of analyzing cardiomyocyte phenotype *in vitro* are present, but each has its own limitations. Physical analysis methods interfere with the cardiomyocyte environment while optical methods have been almost entirely used upon single cell studies. Mechanical contraction is an obvious physiologically relevant endpoint for the analysis of cardiomyocyte tissue maturity. As such, lab efforts have prioritized developing optical analysis of cardiac tissues *in vitro*.

1.2 *Background*

1.2.1 *Heart Disease*

The heart is a structurally specialized muscle that pumps oxygenated blood throughout the body via paced contractions. It possesses a unique design consisting of layers of aligned, rotated cardiomyocyte layers that provide a specialized wringing motion to cardiac contraction[38]. As a critical organ for nutrient and oxygen circulation in the body, damage to the heart can result in a variety of pathologies, both ischemic and non-ischemic.

1.2.2 *Myocardial Infarct*

One critical and relevant injury resulting from ischemia is the myocardial infarction. A coronary artery that supplies blood to the heart tissue itself is occluded. This blockage causes damage to the heart muscle due to a period of hypoxia, resulting in necrotic or infarcted tissue. Given time,

this dead tissue will heal into fibrous scar tissue that lacks the electrical and mechanical properties that functional adult cardiomyocytes contain[26]. The heart has extremely limited regenerative abilities, and as such medical or surgical intervention is often required. Without treatment, an extended length of time can cause a heart with infarcted tissue to suffer further structural damage leading to dilated cardiomyopathy[14,15,26].

Success of clinical treatments for myocardial infarcts is heavily dependent upon the time between the infarct event and the beginning of treatment. That is, the time of hypoxic condition in the infarcted area is critical when observing patient outcomes. Clinical treatments include medicines to lower blood pressure and reduced secondary injury to the heart wall from dilated cardiomyopathy as ventricular remodeling occurs. Surgical interventions such as mechanical ventricular pumps as well as complete transplants are also available. These procedures are highly invasive and require lifelong immune suppression regimens to avoid rejection. The widespread presence of myocardial infarctions in the developed world make MI treatment a top priority for the application of cardiac tissue engineering, along with a host of other cardiac diseases. Engineered tissue provides a chance to study and perform partial tissue transplants to improve patient outcomes without the same level of invasiveness of a total heart transplant[14,15,18].

1.2.3 *Direct Therapy*

Myocardial infarcts leave patches of dead (infarcted) tissue, and many studies have investigated direct application of stem cells and stem cell-derived cardiomyocytes to restore both local function and overall heart function. Shiba et al injected human embryonic stem cell-derived cardiomyocytes into guinea pig MI models to observe healing responses. This study highlighted both the potential for healing, but also noted risks of complications if the injected cells did not

properly couple with the healthy native tissue. Multiple studies show injection of stem cells and stem cell-derived cardiomyocytes to have regenerative effects, but this is thought to be primarily due to cell signals (cytokines) released by the cells, rather than integration of the cells themselves into the damaged tissue[7,18,35,44]. Alternatively, implanting a confluent cardiomyocyte sheet over the infarcted tissue may lead to more effective integration into the heart, as well as partially restored function[44,47]. Cardiac tissue engineering has potential to create engineered tissue constructs that can restore function to damaged cardiomyocyte tissue. The success rate of this functional restoration is highly dependent upon the phenotypic similarity of the engineered tissue to native tissue. Therefore, the ability to make a quantitative assessment of physiological function is critical in this field.

1.2.4 *Disease Modeling*

1.2.4.1 *General Disease Modeling*

Cardiac tissue engineering can be applied toward modeling specific cardiac diseases. In general, animal models or human cell lines are used in conjunction with genetic manipulation to study common cardiomyopathies. Disease models allow scientists the ability to study the effects of disease processes on the scale of both tissues and cells. This has potential to provide insight into the specific mechanisms of various cardiac diseases and can provide specific targets to research for potential medical intervention.

1.2.4.2 *Duchenne Muscular Dystrophy*

Duchenne Muscular Dystrophy (DMD) is a genetic disorder that results in muscular dystrophy due to a mutation in the gene coding for the dystrophin protein. This mutation is X-linked and affects

1 in 3600 boys. The dystrophin protein is a cytoplasmic protein that connects the internal cytoskeleton to the surrounding extracellular matrix. As a result, muscle cells with DMD mutations have limited ability to detect their immediate environment. DMD patients present with a variety of symptoms, including muscle weakness, impaired motor skills, loss of the ability to walk, a higher risk of behavioral disorders, skeletal deformities, and various other outcomes due to deformed muscle fibers. Currently there is no effective cure for DMD, and treatment is aimed at controlling symptoms, especially with regards to respiratory support, as the diaphragm is often affected by the disease process. DMD is a debilitating disease by nature, and as treatments for DMD improve, the cause of death often becomes due to heart failure. Stem cell therapy is a currently researched treatment for DMD, as is utilizing stem cells from DMD-patient cell lines to create *in vitro* disease models. *In vitro* models of DMD tissues can provide information on precisely how the dystrophin mutation affects the maturity, alignment, and phenotype of cardiomyocyte tissues[17,40].

1.2.5 *Drug Screening*

In addition to disease modeling and direct tissue therapy, tissue engineering can be used to create an *in vitro* tool for drug screening. Many current drug studies to test cardiotoxicity utilize either animal cells or single human cells. Animal cells have relevant physiological differences from human cells that call doubt upon the ability to draw conclusions from animal studies and apply them to human cells. Furthermore, single cell studies may be insufficient for drug screenings, especially in the case of cardiotoxicity. Cardiac tissue consists of cells that are coupled both electrically and mechanically so as to contract rhythmically in synchrony. Therefore, many drugs

which may cause arrhythmia in larger cardiac tissues may not result in any noticeable effect when tested upon single cells *in vitro*[1,5,29,48].

1.2.6 *Stem Cell-Derived Cardiomyocytes (SC-CM) and SC-CM Maturity*

Primary rat cardiomyocytes are commonly used for *in vitro* studies of heart cell dynamics due to their availability, wealth of prior research, and robustness. However, they have important physiological differences from human cardiomyocytes that limit the usefulness of applying rat cardiomyocyte test results to humans. Human primary cardiomyocytes are also very difficult to obtain, so human Pluripotent Stem Cell-derived Cardiomyocytes (hPSC-CMs) are an available solution. Pluripotent stem cells have multiple options for cell fates after differentiation. This includes differentiation into cardiomyocytes based on environmental cues, both chemical and physical. These hPSC-CMs can be both embryonic stem cells (ES) harvested from human embryos, or induced pluripotent stem cells (iPSC). iPSCs are differentiated cells that have been de-differentiated back to pluripotency. Both human embryonic Pluripotent Stem Cell derived-Cardiomyocytes (hEPS-CMs) and iPSCs have been shown to display similar phenotypes to adult cardiomyocytes following adequate maturation procedures[32,35,47,49,50]. Maturation procedures for stem cell-derived cardiomyocytes include altering ECM thickness as well as providing electrical stimulation, nanotopography, and mechanical load. Maturity of cardiomyocytes at a structural level is evaluated through the formation of sarcomere structure[19,32,39,47]. The sarcomere is a bundle of proteins in a mature muscle cell that is the functional unit of contraction. It is composed of repeating units of myosin motor proteins and actin filaments. Functional cardiomyocyte maturity is primarily analyzed via contractility and calcium propagation.

1.2.7 *Nanotopography, induced Tissue Alignment, and resultant Stem Cell Maturation*

Nanotopography has been shown to induce cell alignment in cardiomyocyte monolayers by Kim et al. Nanotopographical cues are intended to mimic the high degree of alignment found in the ECM of *in vivo* heart tissue, which shows a high degree of correlation with the orientation of the local cell alignment[38]. Strong alignment has been shown to increase cardiomyocyte maturity in terms of a higher rate of electrophysiological and mechanical coupling in cardiac tissue. This is supported in Kim et al by observation of action potential propagation speed in cardiomyocytes on both nanopatterned and flat substrates[21,22,23,24,25,27]. Action potential propagation speed was shown to be faster along the direction of the nanogrooved substrate. This implies that the cardiomyocytes are showing a greater structural organization along the direction of the substrate. Native cardiac tissue shows a high degree of alignment, and nano-scale patterns imitate *in vivo* ECM in order to produce more mature and well-organized cardiomyocyte tissues. Primary rat cardiomyocytes have been shown by Kim et al to adopt the alignment of nanopatterns, with the greatest degree of alignment on patterns with 800 nm groove widths. Stem cell-derived cardiomyocytes similarly show this behavior and adopt the alignment of the nanopatterned substrates[21,22,23,24,25,27].

1.2.8 Cardiomyocyte Contraction Quantification Methods

Cardiomyocytes, especially those derived from pluripotent stem cells, have a wide range of potential maturity levels that can drastically affect the phenotypic behavior of the cells. Measurement of mechanical contraction of cardiomyocytes is a critical endpoint in determining the maturity of these cells, as the quality of contraction is related to the development of the force generating structures.

1.2.8.1 *Force Transduction*

Several groups have designed mechanical force sensors in order to directly measure cardiomyocyte forces via physical contact.

1.2.8.1.1 *Micro-Scale Strain Gauges*

Multiple groups have utilized specialized custom built micro-scaled strain gauges for measuring the contractile force of cardiomyocytes. Typically, a piece of cardiomyocyte tissue is held between two clamps. As the cells beat, the clamps are displaced. Depending on the type of strain gauge, either the visual displacement of the clamps is measured, or the displacement is detected by the change in the current through a Wheatstone bridge that is functioning as a strain sensor[9,30]. Micro-scale strain gauges are accurate at determining cardiomyocyte force outputs, but require the tissue to be sacrificed as well as removed from an environment similar to what the cells would be in *in vivo*.

1.2.8.1.2 *Micro-Cantilever Arrays*

Micro-cantilever arrays are a physical tool built into the substrate beneath a confluent cell layer *in vitro* with which to measure the force of contraction. A confluent cardiomyocyte monolayer is cultured upon the substrate. The micro-cantilever array appears similar to a rectangular shape cut out on three sides. As the cells contract, they pull up on the cantilever and the cantilever curls upward in the z-direction along the length of the cantilever itself. Based on the Young's modulus of the cantilever material as well as the measured radius of curvature of the cantilever, the displacement of the edge of the cantilever can be determined. Based on the displacement of the cantilever edge, the force exerted upon this device can be calculated[2,36,37]. This device provides

an absolute force measurement, but its accuracy is dependent upon the degree, nature, and quality of focal adhesions present in the cell monolayer.

1.2.8.1.3 *Micro-Post Arrays*

Micro-post arrays are another tool used by multiple research groups that utilizes cantilever beam modeling equations to determine the force of cardiomyocyte contraction. However, micro-post arrays differ in that the beam axis is orthogonal to the contraction axis of the cardiomyocytes. The cardiomyocytes are placed upon a substrate on top of vertical micro-posts. The cardiomyocytes grow and form focal adhesions with the tops of the individual micro-posts. As the cardiomyocytes contract, the micro-posts are deflected by the tension in the focal adhesions. Based upon the Young's modulus, an index of rigidity, the displacement distance, and the dimensions of the micro-posts, the force exerted on the micro-posts can be calculated[41,45,46].

1.2.8.2 *Atomic Force Microscopy (AFM)*

Atomic Force Microscopy (AFM) functions by placing an extremely fine cantilever extremely close to an object, such that motion of the object affects the location of the cantilever by means of electronic repulsion. Typically the location of the cantilever is adjusted using a series of controller servos that monitor the electrical field adjacent to the cantilever. A laser is reflected off of the top of the cantilever beam onto a sensor. This precise location of the laser on the sensor is used to measure the deflection of the cantilever beam in extremely fine detail. The Liau group utilized this method to measure z-directional displacement of the cardiomyocyte membrane[29]. The cantilever was placed above the cardiomyocyte. During contraction, the cardiomyocyte shortened along its major axis and expanded along the orthogonal plane, resulting in vertical displacement

of the AFM cantilever. Assuming a Poisson ratio of ~0.5, the contractile force and displacement could be calculated[11,29].

Other groups have utilized a similar protocol, but physically place the AFM cantilever in contact with the cardiomyocyte membrane perpendicular to the contractile axis of the cell. As the cell contracted, the membrane exerted a torsional force upon the AFM cantilever[11,29]. This resulted in a measurement of the direct force applied in the direction of contraction. However, this may not take into account needle slippage, and this experiment requires the cells to be sacrificed.

1.2.8.3 *Traction Force Microscopy (TFM)*

Traction Force Microscopy (TFM) utilizes the dynamics of a gel substrate beneath the cells in order to measure the contractile force of the cells. TFM has been used by various groups to measure the force exerted by cells on the substrate they rest on, but when applied to cardiomyocytes, can be used to visualize this effect as the cell contracts. The substrate beneath the cell has fluorescent beads bubbled through the material. In a fluorescent microscope, the beads can be captured via video acquisition. The motion of the beads beneath these cardiomyocytes can be used in conjunction with the Young's modulus of the substrate to determine the force that the cardiomyocytes are exerting upon the substrate, and thus the force of contraction. This model is, however, limited by a number of assumptions, primarily involving the variable depths of the fluorescent microbeads as well as the nature of the junction between the focal adhesions and the sarcomere motor units[16,43].

1.2.8.4 *Optical Mapping*

Physical force transducers are effective in measuring absolute force exerted by cardiomyocytes, but they have weaknesses in execution. They require specialized equipment, many of them, such as torsion AFM and micro-scale strain gauges require the tissue sample be sacrificed, and they modify the cell environment from what it would be similar to *in vivo*. In comparison, entirely optical methods, while difficult to obtain absolute force measurements, can provide important, physiologically relevant data relevant to cardiomyocyte maturity.

1.2.8.4.1 *General Optical Methods*

Optical methods of cardiomyocyte contraction analysis provide an advantage in that they preclude the need for specialized equipment. A common method is to use line scans on single cardiomyocytes to track motions along a single axis of either membrane intensity contrast or, if sufficiently developed, sarcomeric structures. Many of these optical methods are specialized for single cell analyses, rather than full tissues[3,20,28].

1.2.8.4.2 *Correlation-Based Tracking*

In correlation-based tracking, a reference video frame is divided into a grid of windows of a set size. Each window is run through a correlation scheme with a second frame. This provides a new location for that window in the second frame (**figure 1**). The correlation equation that each window is analyzed with provides Gaussian correlation peaks. The probabilistic nature of these peaks means that the correlation scheme has subpixel accuracy. Correlation-based image analysis has previously been used for flow analysis in fluidics. This includes primarily applications in wind tunnel data and flow tunnels. However, Particle Image Velocimetry (PIV), a type of Digital Image Correlation (DIC) has been used to analyze migration of endothelial cells in order to model wound

healing[34]. Recently, DIC has been used to analyze the velocity and displacement profiles of adult human cardiomyocytes *in vitro*. However, previous analyses of cardiomyocytes utilizing DIC have been on single cells *in vitro*. Analysis of cardiomyocytes in confluent tissue layers may reveal collective group cell behavior more similar to native cardiac tissue than single cell behavior[3,20,28].

1.3 *Summary*

Tissue engineering of cardiomyocytes requires standardized metrics for maturity analysis. Cardiomyocyte maturity is related to the structural development of the sarcomeric motor units, and thus the quality of mechanical contraction. A number of methods are available to test the contractile properties of cardiomyocytes. Optical methods preclude the need for specialized devices that modify the environment of cardiomyocytes, but have limited prior application to tissue-scale cardiomyocyte constructs. Application of Digital Image Correlation algorithms to cardiomyocyte algorithms can provide practical insight on the collective behavior of these cardiomyocyte tissues.

1.4 *Thesis Outline*

In this thesis we develop the use of Correlation-based Contraction Quantification (CCQ) algorithms that utilize both PIV and DIC open-source software to track contraction motion and strain in cardiomyocytes. We will validate and optimize these algorithms for accuracy and efficiency, then apply them to a case study analyzing induced Pluripotent Stem Cell-derived cardiomyocytes from a human subject with the genetic mutation for DMD.

In chapter 2, we present data on the accuracy and validation of various physiologically relevant endpoints for the CCQ algorithms. CCQ is used to analyze orientation of both primary rat cardiomyocytes and hPSC-CM's on nanopatterned substrates. CCQ is validated in terms of displacement measurements by comparing local CCQ-derived displacement values to displacements derived from micro-post arrays. Beating frequencies are confirmed via a frequency response experiment on primary rat cardiomyocytes. Chapter 2 evaluates the ability of CCQ to detect accurate relevant physiological endpoints of both primary and stem cell-derived cardiomyocytes.

In chapter 3 we apply CCQ to induced pluripotent stem cell-derived cardiomyocytes with a mutation for a DMD phenotype. These stem cell-derived cardiomyocytes are compared to wild type induced pluripotent stem cell-derived cardiomyocytes for their strain behavior as well as their induced-orientation response to nanotopographical cues. Chapter 4 discusses the conclusions of these studies and briefly presents both ongoing and future work.

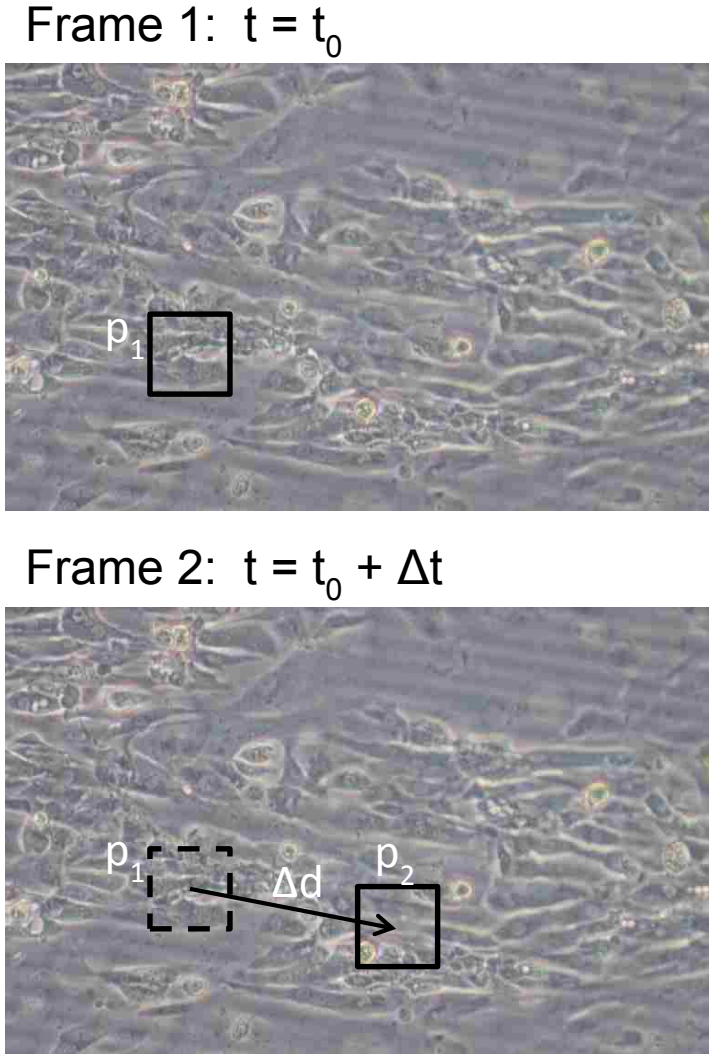

Figure 1. Representation of correlation analysis scheme. P_1 = Interrogation window position 1. P_2 = interrogation window position 2. Δd = Displacement vector.

CHAPTER 2: DEVELOPMENT AND VALIDATION OF CORRELATION-BASED CONTRACTION QUANTIFICATION (CCQ) ANALYSIS

2.1 *Introduction*

In a previous study, PIV analysis has been used to track translational cell motion as well as single cell adult cardiomyocyte contraction *in vitro*. The goal of this project was to develop CCQ analysis specifically for the purpose of analyzing contracting cardiomyocyte monolayers to observe and compare collective behavior in engineered tissues. First, this requires selection of parameters for the DIC and PIV algorithms that will provide accurate final analysis. Next, validation of the CCQ endpoints to ensure accuracy is required. Finally, we will explore some more potential uses of CCQ by conducting a brief drug administration study.

Endpoints from CCQ analysis that require validation include beating frequency, contraction orientation analysis, displacement/velocity analysis, and strain analysis. Beating frequency can be validated by electrical pacing of cardiomyocyte monolayers and single cells *in vitro* at various frequencies. Orientation analysis can be confirmed by analysis of cell monolayers beating on nanopatterned vs. flat substrates. It has previously been established in this lab that nanopatterned substrates lead to highly aligned monolayers in cardiomyocytes compared to random alignment. This will be confirmed with both NRVMs as well as RUES-2 cardiomyocytes. Basic validation for displacement tests include artificial spatial shifts of single brightfield frames of NRVM monolayers both horizontally and vertically a fixed amount. This will show the accuracy of the CCQ analysis as true displacement rises and correlation error grows. Displacement

will be further validated by analysis of cardiomyocytes on microposts via correlation of CCQ displacement to local micropost displacement.

2.2 *Materials and Methods*

Fabrication of Nanopatterned Substrates

Norland Optical Adhesive (NOA) 76 substrates were used as the substrate material in each validation experiment in a method previously established in the Kim laboratory. NOA 76 nanopatterned substrates were fabricated using capillary force lithography. 40 µl polyurethane acrylate (PUA) was dropped onto the first generation silicon master nanopatterns. A sheet of transparent polyester (PET) was placed over the PUA and then cured approximately 10 cm below a 20 W UV light for 30 seconds. After curing, the PET film is removed, and the PUA/PET was cured under UV for 12 hours. 10 µl NOA 76 polymer was dispensed onto a treated glass slide, which was then placed on the nanopatterned PUA/PET surface. This was then UV cured for 50 seconds before the glass was removed. The NOA-coated glass surface was fixed to the bottom of a 35 mm culture dish with a 13 mm well using the adhesive NOA 83, and cured for twenty minutes in the fusion device. After treatment the substrates were sterilized under UV light for approximately one hour before a 10 ug/cm^2 solution of fibronectin was added. This solution was allowed to sit for one night to deposit a fibronectin coat to aid cell adhesion. The micropost grid used to implement the displacement correlation algorithms was a PDMS mold created from a silicon master also using capillary force lithography.

NRVM Isolation

Neonatal Rat Ventricular Myocytes (NRVMs) were the primary cell source for stimulation and norepinephrine experiments. NRVM acquisition is then conducted via a method previously implemented in the Kim lab and adapted from a process used in the Regnier lab. NRVM acquisition occurs via heart removal from sacrifice neonatal rats. Hearts are placed into Ads buffer solution where the aorta is detached. Ventricular myocardium was then further mechanically separated to increase cell digestion efficiency. The myocardium fragments are then placed in a digest solution consisting of Ads buffer, collagenase II, and protease XIV. From the supernatant, cells were isolated via centrifuge and supernatant aspiration. The cells were then suspended in media. This process was repeated 3x to increase NRVM yield.

Cell Culture

NRVMs and RUES-2 cardiomyocytes were grown at 37^0 C for seven days before the beginning of each experiment. NRVMs for confluent monolayer experiments were seeded at a density of 500,000 cells/cm^2. NRVM media was changed on alternating days. Media consisted of DMEM, HEPES, M199, Horse Serum, Fetal Bovine Serum, and Pen-Strep, with Ara-C used to reduce fibroblast populations in culture and promote contractions.

Microscopy and Data Acquisition

Data was acquired via Nikon-based brightfield avi-acquisition. Videos were captured at a framerate of 15 frames per second was established for general analysis.

Structural Analysis

A custom MATLAB code utilizing a Hough transform is used on a representative image of the brightfield frames in question. This transform finds the orientation of the cell edges to provided information on the structural alignment of these cells independent from the contractile motion.

CCQ Analysis—General

Before CCQ analysis, videos were parameterized to general standards to promote consistent analysis. Prior to analysis units are converted to microns via the scaling ratio for the magnification used during data acquisition.

CCQ Analysis—Orientation Analysis

CCQ Analysis provides a vector map for each frame of analyzed video. The contractile axis is used rather than the particular angle in order to group together uniaxial motion. That is, contraction and relaxation is considered the same angle of motion as it is along the same axis. Therefore, the vector angle range was fixed to –pi/2 to pi/2 by adding pi to each vector angle that was below –pi/2, and subtracting pi from each vector angle that was above pi/2. A temporal average of the vector field angles is taken and visualized on a heat map as a representative image. A polar histogram is presented containing the temporal average of vector fields of multiple movies to provide a realistic assessment of the entirety of the data.

Micropost Displacement Measurements

To calculate the displacement of microposts, microposts were individually analyzed in MATLAB. The microposts were tracked using a Circular Hough Transform (CHT). The CHT is computed by finding an edge, then attempting to find more edges in a circle around the initial point at a fixed

designated radius. Once this second edge is found, the CHT searches out more edges at a fixed radius using the new second edge as a center until a complete circle is found. This eventually provides the center and radius of a circle, in this case the tops of a specific micropost.

CCQ Analysis—Displacement/Velocity Analysis

PIV analysis in the CCQ algorithm produces a vector field between each adjacent movie data frames detailing the results of the correlation analysis. These are averaged spatially to provide a time lapse displacement plot. To validate the displacement analysis, PIV was run on a micropost device seeded with primary rat cardiomyocytes, and the local PIV displacement was compared to the micropost displacements. A second order low-pass Butterworth filter was run on both displacement calculations in order to filter out high-frequency noise. A correlation coefficient was calculated between PIV and micropost displacements (**figure 2a, b**).

CCQ Analysis—Strain Analysis

DIC-based strain analysis performs a correlation-based method similar to PIV. After this calculation, by integrating spatially percent changes/strains were determined. Strains were visualized using heat maps during contraction. Spatial averages of strains were used to provide a time lapse of strains (**figure 2c)**.

Statistical Analysis

Alignment of cardiomyocyte contractions can be estimated by comparing the differences in variability of the contraction vector angle distributions. This is achieved by using an F-test at $\alpha = 0.05$.

2.3 *Results/Discussions*

Validation of Displacement

Artificial translational shifts between 1 and 30 pixels were conducted in both the x and y directions. Root mean square error between the artificial shift and the measured displacement increased as the displacement grew above twenty pixels. Comparing three methods of image contrast pre-processing: a control, a local normalization filter, and global intensity normalization resulted in the local normalization filter producing the smallest root mean square error, followed by the global intensity filter. The control with no pre-processing showed higher RMS error compared to the local normalization filter and global intensity normalization (**Figure 3**). The RMS error shows that average error is on the scale of approximately one tenth of a pixel.

Additionally, CCQ displacement data was compared to displacement data obtained locally by primary rat cardiomyocytes on a micropost array. The local CCQ-calculated displacement immediately adjacent to the micropost arrays was on the same order of magnitude of displacement. The correlation coefficient between local CCQ displacement and micropost deflection via circular Hough transform was calculated at six different moving microposts. The average correlation coefficient was calculated to be 0.72. This suggests a moderately strong correlation between micropost deflection measurements and CCQ displacement measurements, thus further validating the accuracy of the CCQ tracking methodology (**Figure 4**).

Validation of Orientation

Nanopatterned substrates revealed a high degree of structural alignment at 800 nm compared to a flat substrate for both primary rat cardiomyocytes (**Figure 5a, b**) as well as human embryonic stem

cell-derived cardiomyocytes (**Figure 6a, b**). Nanopatterned substrates also appear to show a high degree of contractile alignment (**Figure 5c, 5d, 6c, 6d)**. The central line in each polar histogram is representative of the average angle, and the length is inversely related to the variation of the distribution; the length represents an index of alignment. The F-tests showed sufficient evidence to reject the null hypothesis that the flat substrates did not show larger variation than the nanopatterned substrates. This is evidence that the cell monolayers grown upon nanopatterned substrates show greater alignment than those grown upon flat substrates. This agrees with both the structural alignment and prior work.

2.4 *Summary*

Here we present CCQ as a method of effectively and accurately analyzing cardiomyocyte contraction *in vitro*. This study aimed to expand the use of correlation based analyses into the monolayer scale by analyzing and validating specific relevant physiological endpoints. This includes beating frequency, beating displacement, contraction orientation, and strain. By correlating CCQ displacement data with micropost motion, we validate the displacement measurements' accuracies based on the correlation algorithm applied to brightfield microscopy videos. CCQ analysis to measure cardiomyocyte alignment on patterned substrates was used to analyze both primary rat cardiomyocytes as well as human embryonic stem cell-derived cardiomyocytes. CCQ analysis confirmed previous studies' assessments that nanopatterned substrates promote cardiomyocyte monolayer alignment over flat substrates. This study showed that CCQ is an effective tool for measuring monolayer alignment, contractile displacement, beating frequency, and strain. These are physiologically relevant endpoints for measuring maturity and phenotypic function of cardiomyocyte monolayers.

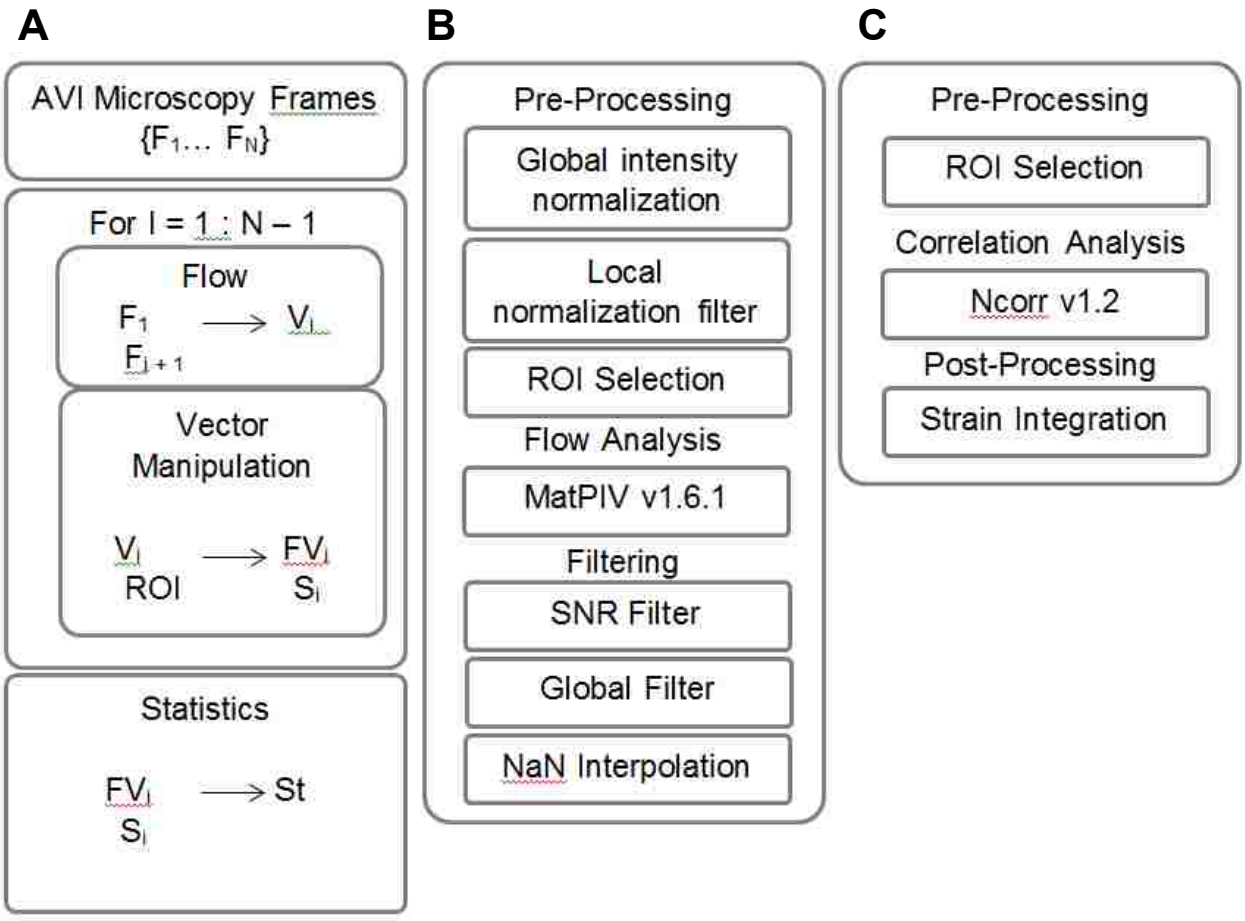

Figure 2. General algorithm and workflow of correlation scheme. General algorithm (a) of correlation analysis: F = frame, V = velocity field, ROI = Region of Interest, FV = Field Velocity, S = Strain, St = Statistics. Workflow process for PIV (b) and strain (c) analysis code.

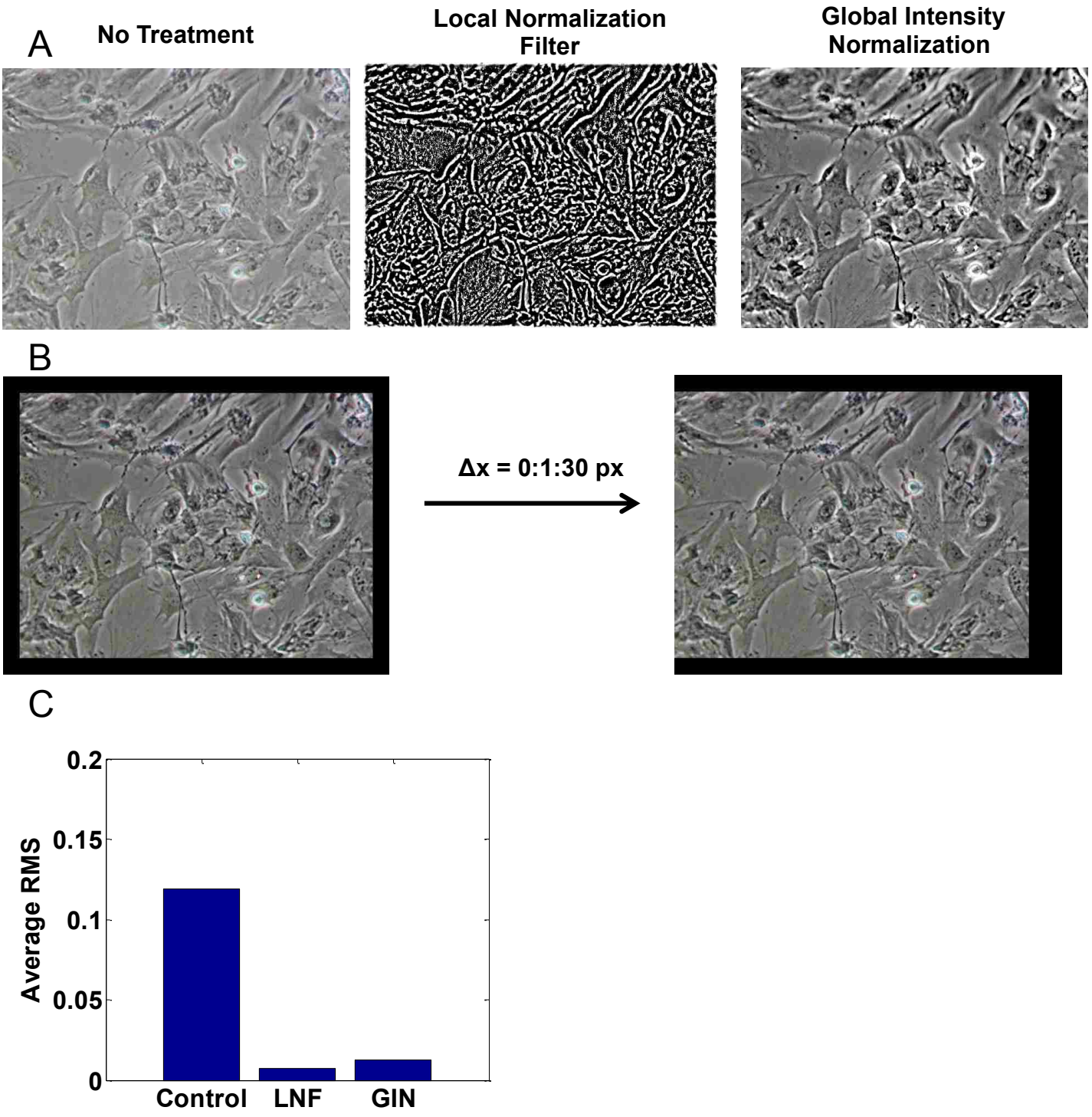

Figure 3. Validation testing of multiple pre-processing contrast adjustments. Representative images of the control treatment, the local normalization filter treatment, and the global intensity normalization (a). Representation of a translational shift (b) for testing. Average RMS for various pre-processing treatments.

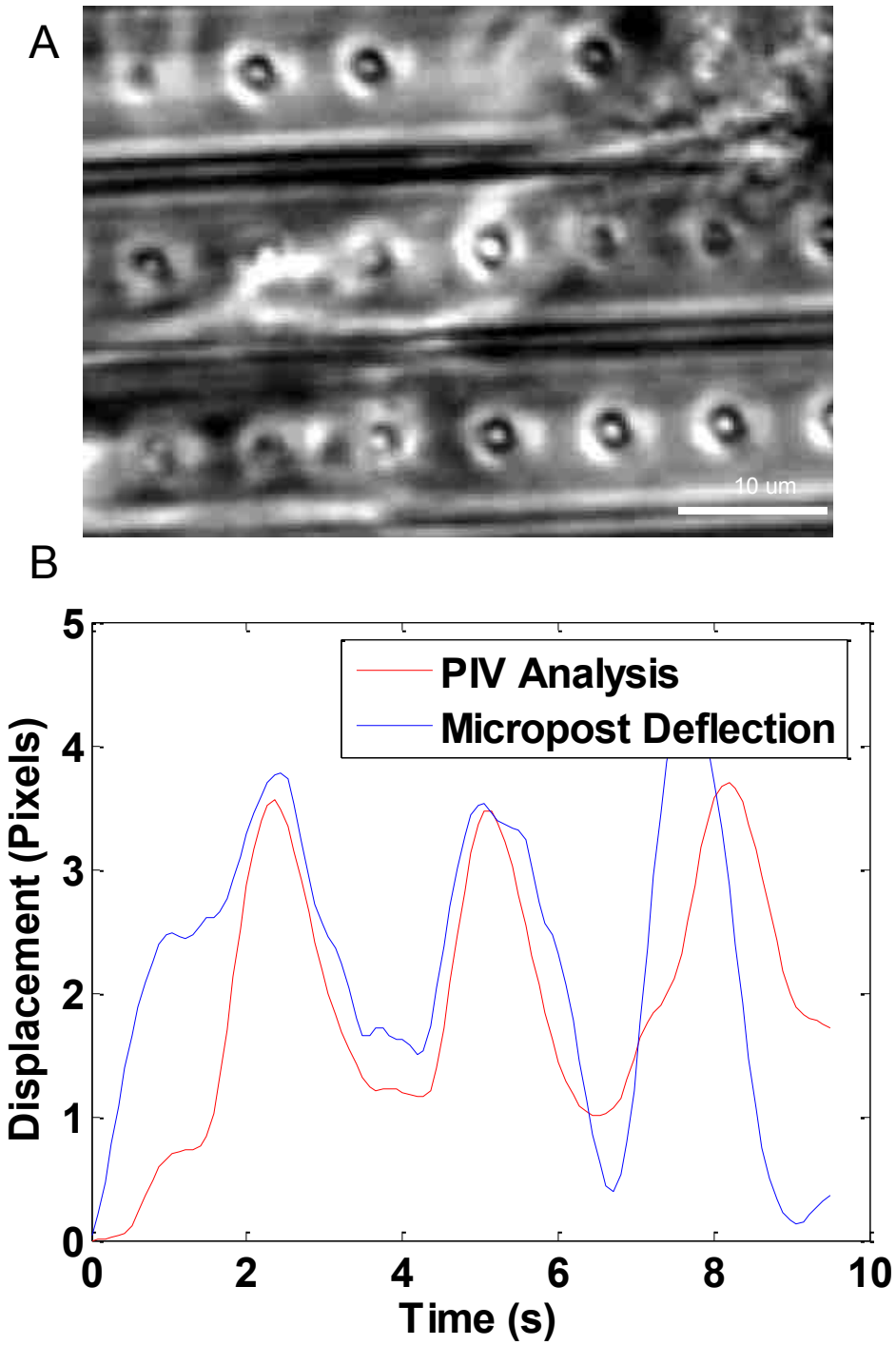

Figure 4. Validation of CCQ displacement based on micropost displacement correlation. A brightfield image of primary rat cardiomyocytes resting upon a micropost-pattern hybrid substrate design (a). Representative plot of micropost deflection compared to local PIV displacement. Average Correlation Coefficient = 0.72.

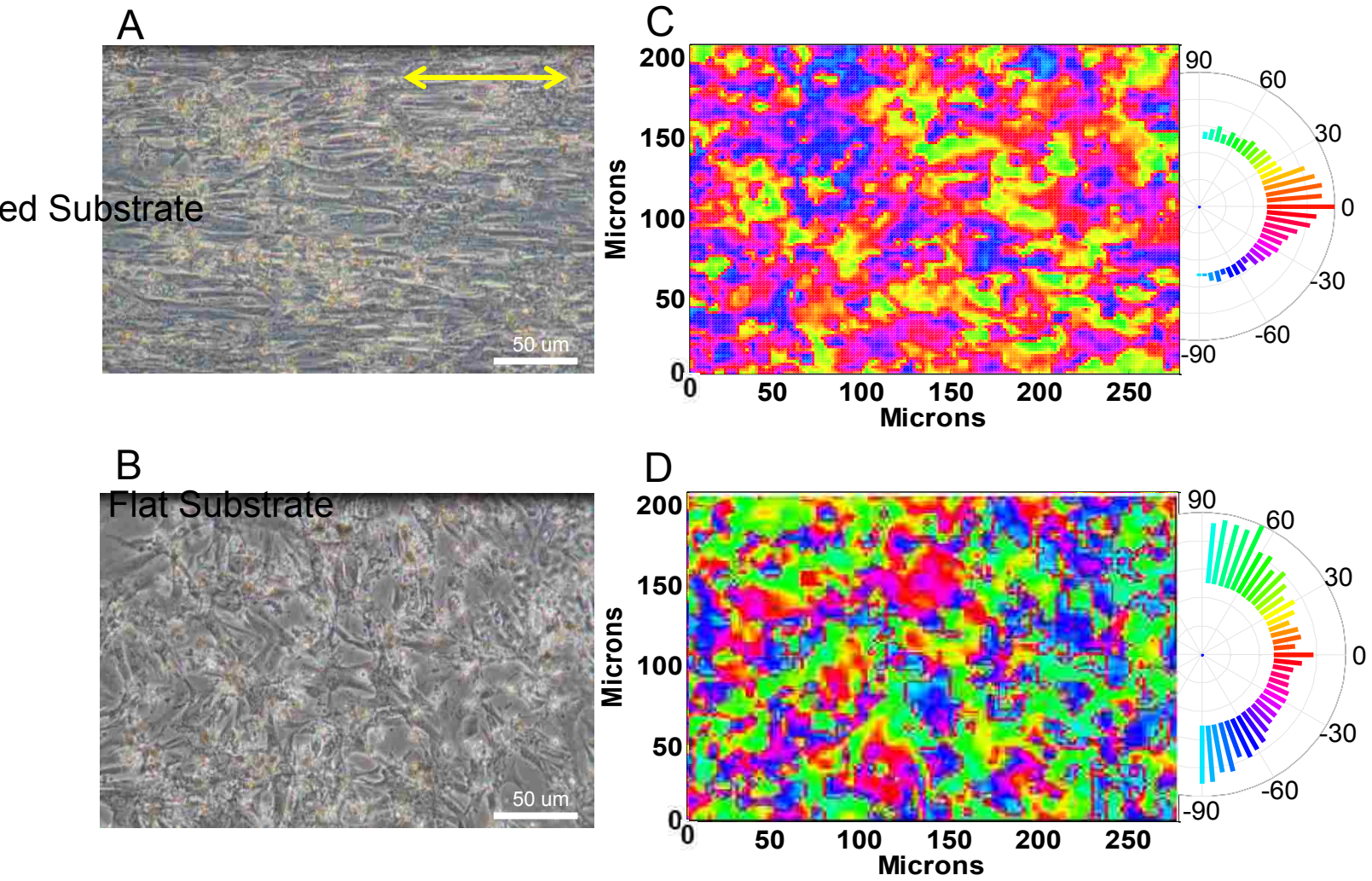

Figure 5. Primary cardiomyocyte alignment analysis on nanopatterned and flat substrate. Representative image of primary rat cardiomyocytes cultured for 7 days on 800 nm NOA 76 substrates (a) and flat substrates (b) with the nanopattern direction marked. Hough transform structural alignment analysis showed an average orientation angle of -0.89 degrees from the horizontal with a variation of 5.6 in the patterned substrate brightfield image. A hough transform structural alignment analysis showed an average orientation angle of 1.82 degrees from horizontal, with a variation of 173.06. A representative heatmap displaying orientation angles (c, d) and a polar histogram with the compiled angle data from multiple videos (n = 3).

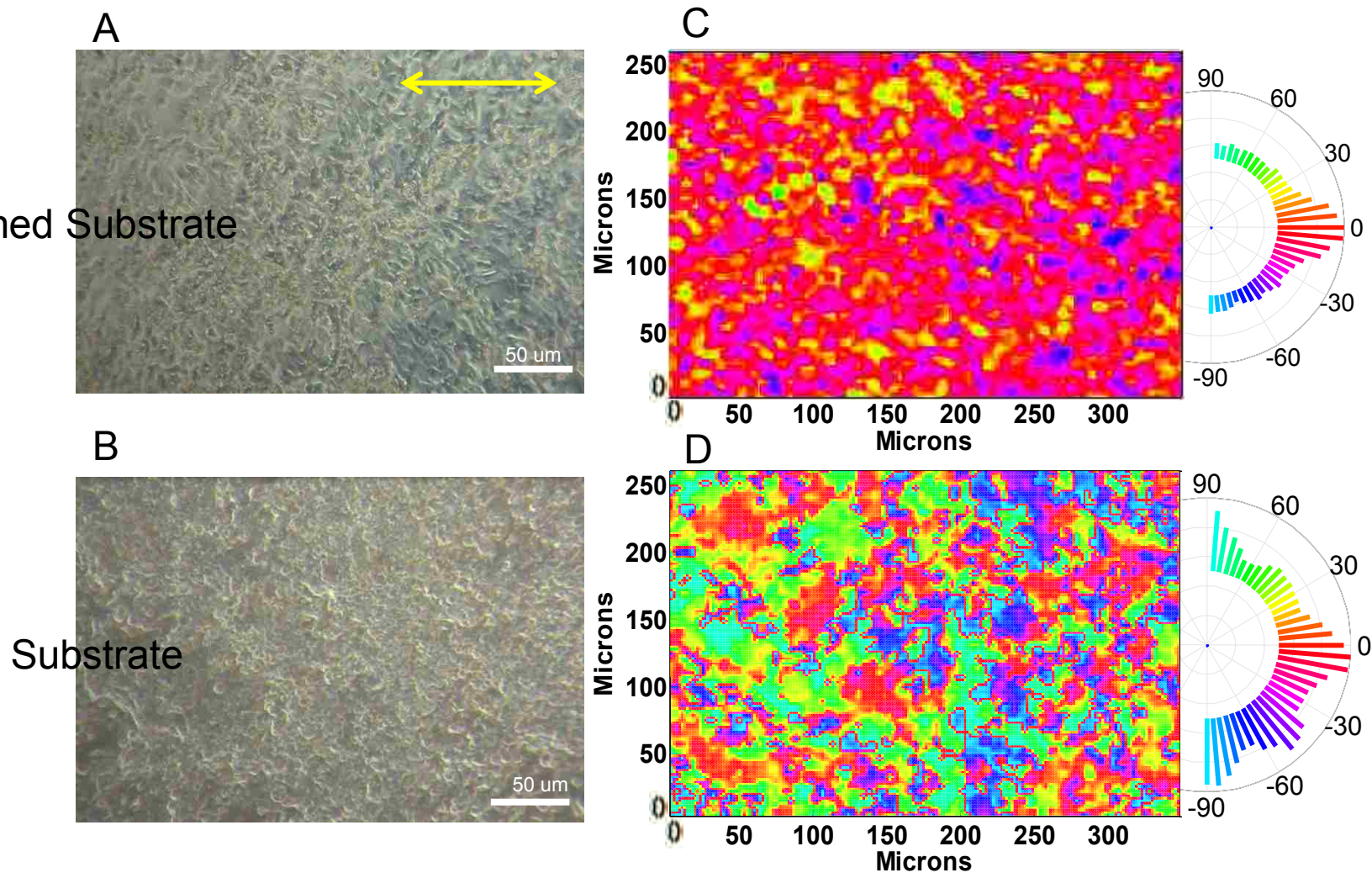

Figure 6. Human embryonic stem cell-derived cardiomyocyte alignment analysis on nanopatterned and flat substrate. Representative image of human embryonic stem cell derived-cardiomyocytes cultured for 7 days on 800 nm NOA 76 substrates (a) and flat substrates (b) with the nanopattern direction marked. Hough transform structural alignment analysis showed an average orientation angle of 1.96 degrees from the horizontal with a variation of 1142.3 in the patterned substrate brightfield image. A hough transform structural alignment analysis showed an average orientation angle of 1.00 degrees from horizontal, with a variation of 825.9. A representative heatmap displaying orientation angles (c, d) and a polar histogram with the compiled angle data from multiple videos (n = 3).

CHAPTER 3: CASE STUDY—DUCHENNE MUSCULAR DYSTROPHY

3.1 *Introduction*

Duchenne Muscular Dystrophy is a disease affecting the mechanisms of cells that regulate the contact between that cell and its environment, specifically the dystrophin protein. Prior research in this lab has shown that cardiomyocytes cultured on nanopatterned substrates show anisotropic behavior by forming aligned monolayers. The disruption of the dystrophin protein pathway would suggest that DMD-phenotype cells may show limited or no anisotropic behavior when grown on nanopatterned substrates. In order to study the behavior of DMD-phenotype cardiomyocytes, CCQ analysis will be performed upon induced pluripotent stem cells (iPSC) from humans with WT dystrophin genes as well as the DMD mutation. Strain and alignment between the DMD and WT cells will be compared.

3.2 *Materials and Methods*

Fabrication of Nanopatterned Substrates

Norland Optical Adhesive (NOA) 76 substrates were used as the substrate material in each validation experiment in a method previously established in the Kim laboratory. NOA 76 nanopatterned substrates were fabricated using capillary force lithography. 40 µl polyurethane acrylate (PUA) was dropped onto the first generation silicon master nanopatterns of size 800 nm with a 1:1 ratio of groove to peak width. A sheet of transparent polyester (PET) was placed over the PUA and then cured approximately 10 cm below a 20 W UV light for 30 seconds. After curing, the PET film is removed, and the PUA/PET was cured under UV for 12 hours. 10 µl NOA 76 polymer was dispensed onto a treated glass slide, which was then placed on the nanopatterned

PUA/PET surface. This was then UV cured for 50 seconds before the glass was removed. The NOA-coated glass surface was fixed to the bottom of a 35 mm culture dish with a 13 mm well using the adhesive NOA 83, and cured for twenty minutes in the fusion device. After treatment the substrates were sterilized under UV light for approximately one hour before a 10 ug/cm^2 solution of fibronectin was added. This solution was allowed to sit for one night to deposit a fibronectin coat to aid cell adhesion.

iPSC Differentiation

Urine-derived cardiomyocytes were collected from urine specimens via centrifuge, then washed with PBS and plated in keratinocyte serum-free medium (KSFM) and DMEM/10%FBS. The iPSCs were differentiated based on an established protocol dictated by Laflamme et al and Guan et al. iPSC colonies were detached by 10 minute incubation with Versene. These colonies were triturated into a single-cell suspension, then seeded on Matrigel-coated plastic dishes at 250,000 cells/cm^2 in mTeSR1 medium. After four days of culture, medium was switched to RPMI-1640 to begin differentiation. The new medium was supplemented with 2% insulin-reduced B27 and L-Glutamine.

Cell Culture

WT and DMD iPSC-CMs were cultured on both 800 nm 1:1 nanopatterned and flat NOA76 substrate. Media was changed every other day. Video was taken on day 14 of culture.

CCQ Analysis—Orientation Analysis

CCQ Analysis provides a vector map for each frame of analyzed video. The contractile axis is used rather than the particular angle in order to group together uniaxial motion. That is, contraction and relaxation is considered the same angle of motion as it is along the same axis. Therefore, the vector angle range was fixed to –pi/2 to pi/2 by adding pi to each vector angle that was below –pi/2, and subtracting pi from each vector angle that was above pi/2. A temporal average of the vector field angles is taken and visualized on a heat map as a representative image. A polar histogram is presented containing the temporal average of vector fields of multiple movies to provide a realistic assessment of the entirety of the data. A quantitative assessment of the orientation distribution was taken by taking the mean and standard deviation, as well as by conducting a chi square test to test for a uniform distribution.

CCQ Analysis—Strain Analysis

DIC-based strain analysis performs a correlation-based method similar to PIV. After this calculation, by integrating spatially percent changes/strains were determined. Strains were visualized using heat maps during contraction. Spatial averages of strains were used to provide a time lapse of strains.

Statistical Analysis

A chi-square test run at 5% significance was utilized to quantify uniformity in alignment distributions. This test was calculated using MATLAB.

3.3 *Results/Discussions*

We present the analysis of induced pluripotent stem cell-derived cardiomyocytes of both DMD and wild type lineages. By analyzing the strain response of these cells during contraction, it is possible to assess both collective and individual behavior in cardiomyocyte tissues with the dystrophin mutation. This also allows direct comparison of contractile phenotypes between DMD and WT iPSC-derived cardiomyocytes.

Orientation Analysis

Both DMD and WT cardiomyocytes showed increased alignment in the direction of the 800 nm nanogrooves when cultured on nanopatterned substrate. These cells showed no directionality when grown on flat substrates. The DMD cardiomyocytes showed greater variation, and lower alignment in contraction angles on the nanopatterned substrates compared to the cardiomyocytes (**figure 7c, 7d, 8c, 8d**). The nanopatterned substrates appear to show lower contraction and relaxation velocities than the flat substrates, and the WT cells appear to show lower contraction and relaxation velocities than the DMD cells. This can be explained by a lack of mature focal adhesions to the substrate in the flat and DMD cells, rather than an immaturity of sarcomeric development in the nanopatterned or WT cells. The F-tests showed that each nanopatterned group showed significantly lower variation than the flat substrate with the same cell condition at the 5% significance level. The F-tests also showed that the nanopatterned DMD group showed higher variation than the nanopatterned WT group. This information can be interpreted as the flat substrates showing less alignment than the nanopatterned substrates overall, and the DMD nanopatterned group showing less alignment than the WT nanopatterned group.

Dynamic strain Analysis

Strain analysis performed on the DMD and WT cardiomyocytes provided insight into the nature of the monolayer contractions. During moments of contraction, patterns of alternating positive (cell stretching) and negative (cell contraction) strain occur. The x-component strain shows vertical streaking (**figure 9b**, **10b**), while the y-component strains show horizontal streaking (**figure 9c, 10c)**. This is logical due to the fact that as cells contract in a certain direction, in a confluent monolayer some regions will need to stretch. The degree of streaking may indicate some index that represents how well the cells are coupled mechanically and electrically. Preliminary evidence suggests that the DMD-type cells show less organized streaking. However, pattern recognition taken using a 2-D fft had insufficient window size to reveal a significant difference in the contraction patterns. Further research should investigate larger fields of view so as to more easily and more accurately visualize recurrent spatial frequencies in this behavior.

3.4 *Summary*

Here we present CCQ in a specific case study of cells with Duchenne Muscular Dystrophy mutations. Utilizing CCQ in a specific instance of a study of induced pluripotent stem cells with both wild type and diseased phenotypes both provides valuable information with regards to the disease phenotype, as well as further validates and broadens the scope of the software. The study investigated orientation analysis and strain analysis of DMD and WT-iPSC-CMs on both patterned and flat substrates. DMD-phenotype cardiomyocytes showed alignment on nanopatterns, but to a lesser degree than the WT-phenotype cells. This suggests some sort of compensatory system or secondary ECM-sensing mechanism. Strain analysis showed higher organization in strain formation in the WT cells compared to the DMD cells, and on the nanopatterned substrates

compared to the flat substrates. Strain formation shape could be an interesting subject of further study, both in terms of cell maturity as well as in the field of DMD research.

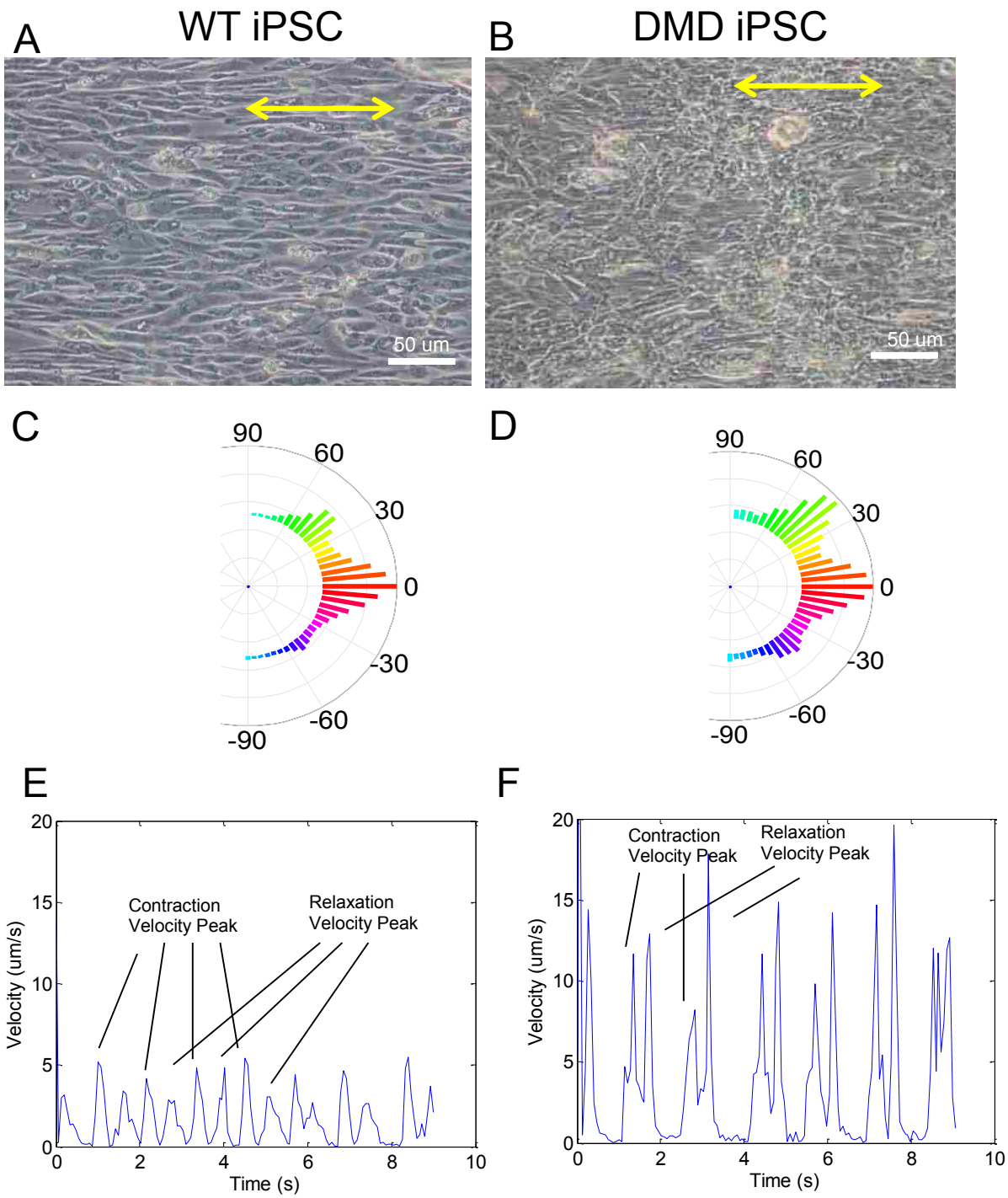

Figure 7. WT and DMD phenotype human induced pluripotent stem cell-derived cardiomyocyte alignment analysis on nanopatterned substrate. Representative image wild type (a, c, e) and DMD iPSC-CMs (b, d, f) cultured for 14 days on 800 nm NOA 76 substrates with the nanopattern direction marked (a, b). Hough transform structural analysis of the brightfield image reveals a mean orientation angle of -1.02 degrees from the horizontal in the WT group, with a variation of 14.82. This analysis reveals a mean orientation angle of -0.57 degrees from horizontal in the DMD group, with a variation of 21.72. A polar histogram with the compiled angle data from multiple videos (n = 3) (c, d). A time lapse of the contraction and relaxation velocity of the beating field of view (e, f).

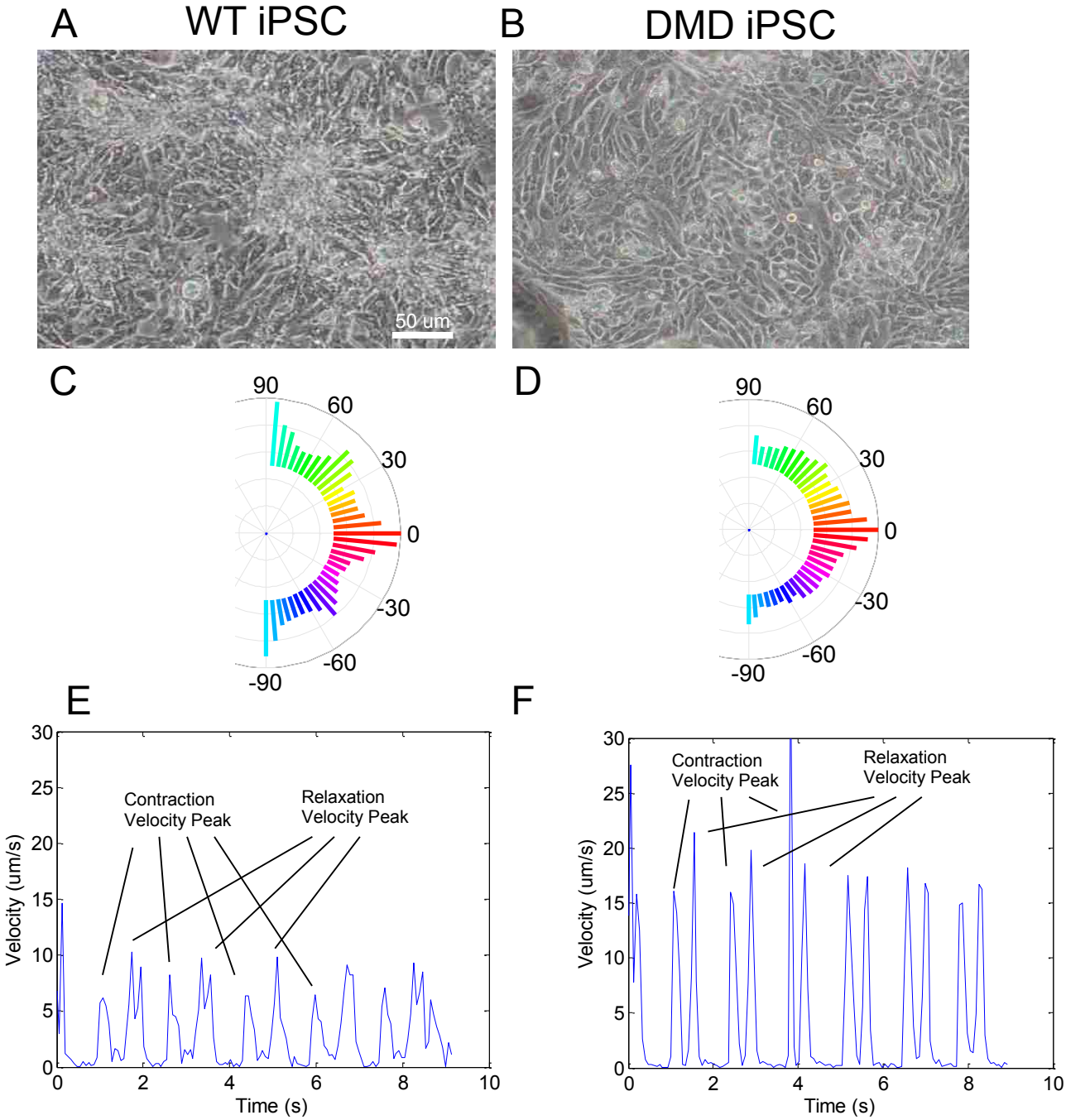

Figure 8. WT and DMD phenotype human induced pluripotent stem cell-derived cardiomyocyte alignment analysis on flat substrate. Representative image wild type (a, c, e) and DMD iPSC-CMs (b, d, f) cultured for 14 days on 800 nm NOA 76 substrates with the nanopattern direction marked. A Hough transform structural orientation analysis of the brightfield image calculated a mean orientation angle at 4.93 degrees from the horizontal axis with a variation of 1108.1 for the WT flat group. A Hough transform structural orientation analysis of the brightfield image calculated a mean orientation angle at 5.48 degrees from the horizontal axis with a variation of 1071.7 for the DMD flat group. A polar histogram with the compiled angle data from multiple videos (n = 3) (c, d). A time lapse of the contraction and relaxation velocities of the field of view (e, f).

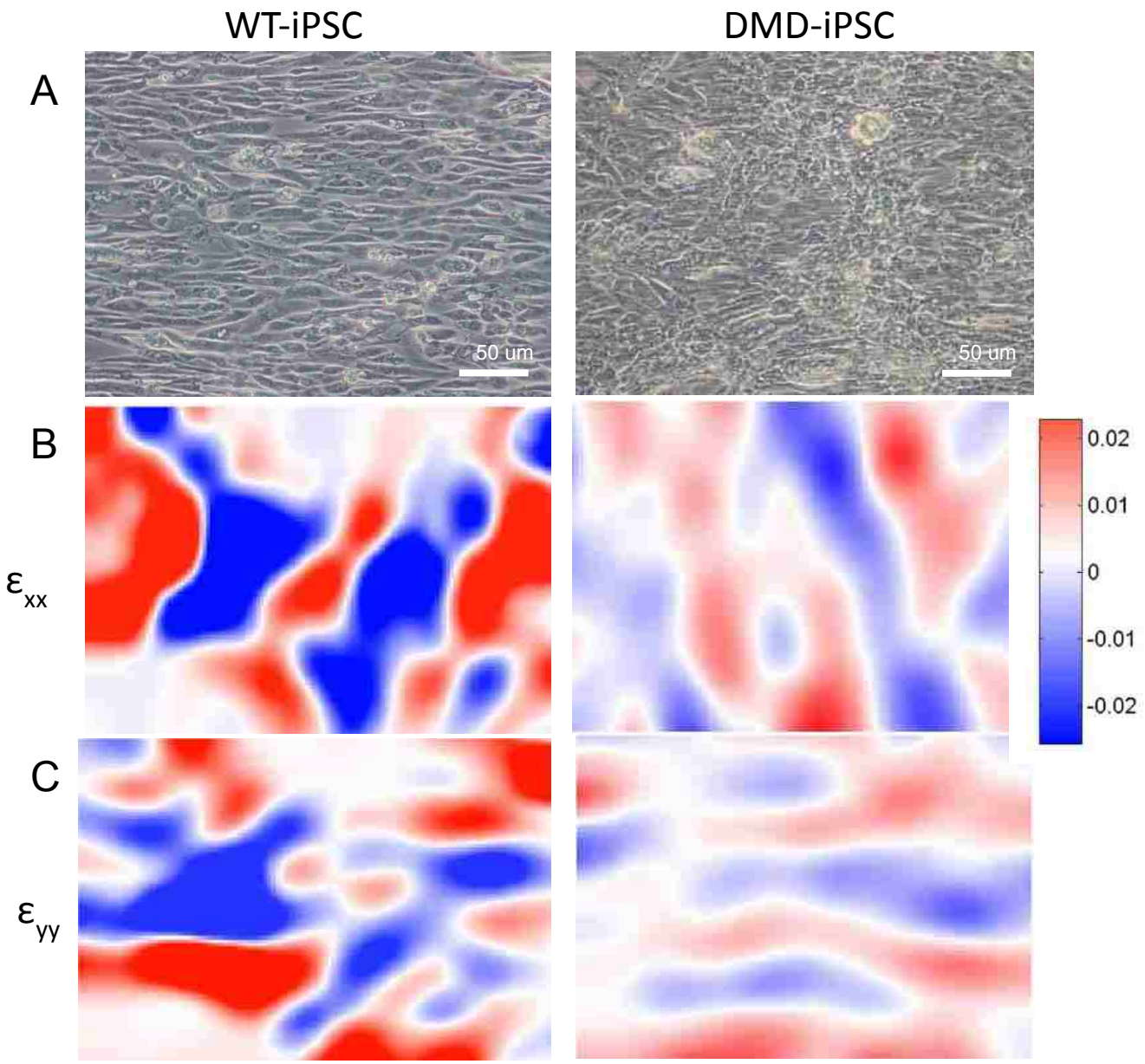

Figure 9. Strain analysis during peak contraction of DMD and WT-iPSC-CMs on nanopatterned substrate. Representative brightfield image of DMD and WT iPSC-CMs on nanopatterned substrates (a, b). DMD and WT iPSC-CMs exhibit streaking contractile and stretching behavior, with vertical streaks in the x component (b) and horizontal streaks in the y component (c)

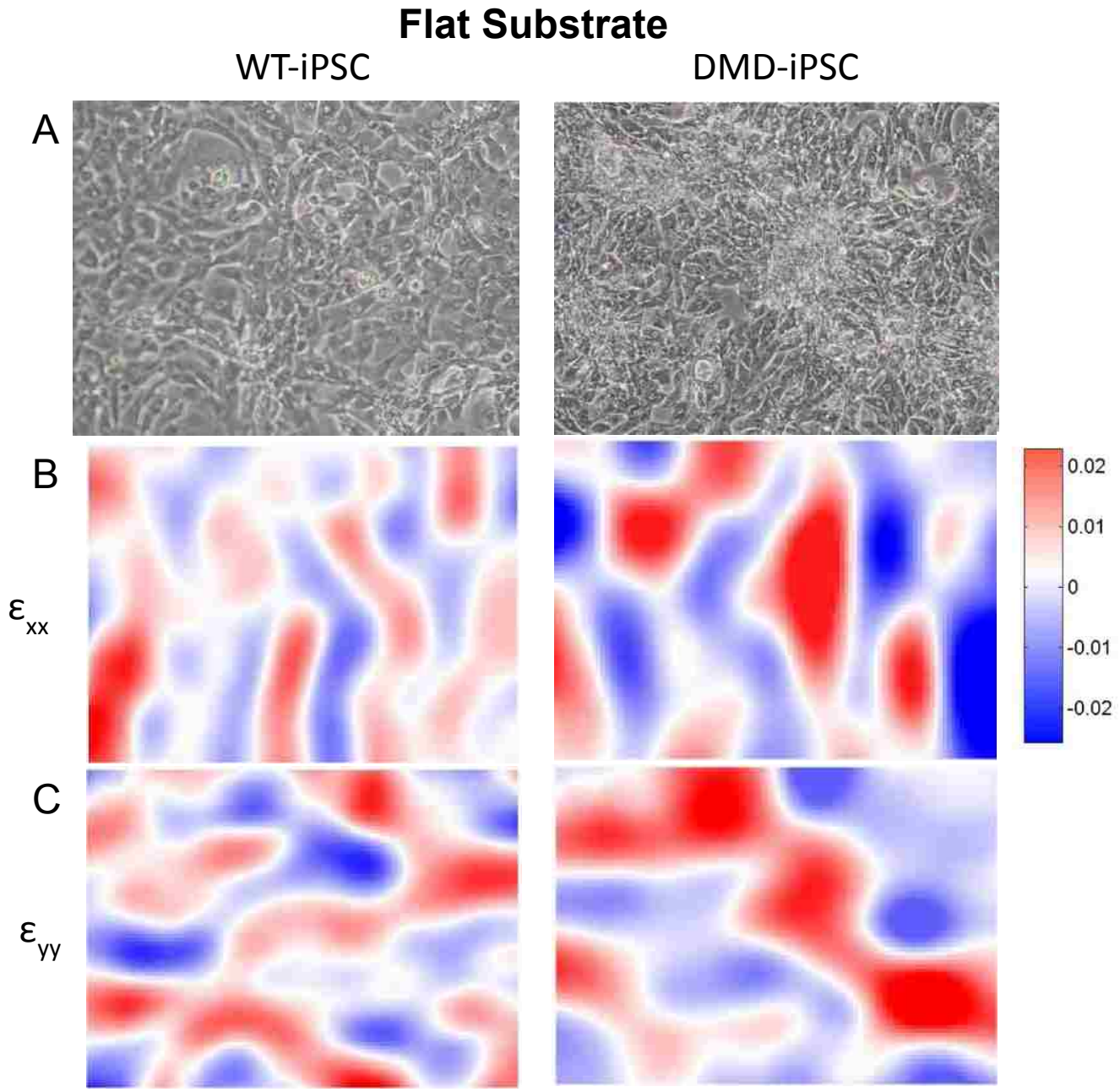

Figure 10. Strain analysis during peak contraction of DMD and WT-iPSC-CMs on flat substrate. Representative brightfield image of DMD and WT iPSC-CMs cultured on flat substrate (a, b). X-directional strain (b) and y-directional strain (c) continue to show patterns of negative and positive strain.

CHAPTER 4: CONCLUSIONS

Initially, we developed Correlation-based Contractile Quantification (CCQ) as a method to use correlation-based image analysis to provide physiologically relevant endpoint for providing information on the behavior and maturity of beating cardiomyocytes *in vitro*. CCQ provides contraction displacement data, contraction orientation alignment data, secondary data based off of displacement (e.g. beating frequency and beating velocity), and strain data along the x axis, y axis, and xy (twisting) axis. We demonstrate validity of displacement and orientation data by comparing to well-known cardiomyocyte behaviors. Preliminary experiments to determine that brightfield video had sufficient contrast to be properly analyzed by correlation-based image analysis determined that global intensity normalization and local normalization filters boosted CCQ accuracy. Validity of displacement was established by correlating CCQ-derived displacement data to independently gathered displacement data based on micropost deflection *in vitro*. Validity of orientation analysis was established by observing primary rat cardiomyocyte monolayers contract on nanopatterned and flat substrates. Cardiomyocytes have been established to align when cultured on nanopatterns, and CCQ orientation analysis confirmed this trend. Strain analysis is based off of spatial integration of displacement data, and is therefore validated by the displacement accuracy. Human embryonic stem cell-derived cardiomyocytes were studied in addition to primary rat cardiomyocytes in order to confirm the possibility of broad application of CCQ analysis. Due to its heavy reliance on particle density and intensity gradients, it was necessary to confirm that superficial differences in cell appearance would not limit or reduce CCQ accuracy.

Next, we applied CCQ analysis to an *in vitro* disease model of Duchenne Muscular Dystrophy, a genetic disorder that damages or removes the dystrophin protein. The dystrophin

protein is a critical piece of the cellular mechanism that connects actin filaments in the cell cytoskeleton to the cell ECM. Without this protein, we expected to see reduced or absent alignment capabilities or alternative compensatory mechanisms. CCQ analysis demonstrated decreased, but still significant alignment in the DMD iPSC-CMs, compared to greater alignment of the WT iPSC-CMs on nanopatterned substrates. Neither cell line showed alignment on flat substrate. Dynamic strain analysis revealed formation of unique patterns of positive and negative strain forming during cardiomyocyte contraction. This took the form of vertical streaks of positive and negative strain when observing x-directional strain and horizontal streaks when observing y-directional strain. This organization decreased on flat substrates, as well as with DMD cells compared to WT cells. This is an excellent basis for future research, as a larger field of view from stitched images could reveal post-processing possibilities as large-scale spatial 2D Fourier transforms could be performed on these patterns to provide some index of the quality of contraction. Further research could also look at differentiating single cell behavior compared to collective behavior in terms of strain.

In this thesis, we have developed a platform for rapid analysis of cardiomyocyte monolayers that precludes the need for specialized equipment, while still providing physiologically relevant endpoints for quantification. The CCQ methodology has improved upon the limitations of previous optical methods, which have primarily focused on individual cardiomyocyte studies. Applying CCQ to larger tissue constructs allows analysis of both individual cell and collective tissue behavior based on individual region of interest study. CCQ has shown itself to be an effective tool with broad application, and will greatly accelerate the quantitative analysis of cardiomyocyte monolayers.

VITA

Samuel Frankel was born in Virginia and raised in Denver, Colorado. He earned in a Bachelor's of Science in Bio-engineering from the University of Washington in 2013. He earned a Master's of Science in Bio-engineering from the University of Washington in 2014.

References

1. Aci, M. I. P., Yttinen, J. A. R. I. H., & Eta, K. A. A. A. (2013). Computational Models of Ventricular- and Atrial-Like Human Induced Pluripotent Stem Cell Derived Cardiomyocytes. *Annals of Biomedical Engineering*. doi:10.1007/s10439-013-0833-3
2. Agarwal, A., Goss, J. A., Cho, A., McCain, M. L., & Parker, K. K. (2013). Microfluidic heart on a chip for higher throughput pharmacological studies. *Lab on a Chip*, *13*(18), 3599–608. doi:10.1039/c3lc50350j
3. Ahola, A., Kiviaho, A. L., Larsson, K., Honkanen, M., Aalto-Setälä, K., & Hyttinen, J. (2014). Video image-based analysis of single human induced pluripotent stem cell derived cardiomyocyte beating dynamics using digital image correlation. *Biomedical Engineering Online*, *13*, 39. doi:10.1186/1475-925X-13-39
4. Asfaw, M., Alvarez-lacalle, E., & Shiferaw, Y. (2013). The Timing Statistics of Spontaneous Calcium Release in Cardiac Myocytes. *PloS One*, *8*(5). doi:10.1371/journal.pone.0062967
5. Baudenbacher, F., Schober, T., Pinto, J. R., Sidorov, V. Y., Hilliard, F., Solaro, R. J., … Knollmann, B. C. (n.d.). Myofilament Ca 2 + sensitization causes susceptibility to cardiac arrhythmia in mice. doi:10.1172/JCI36642.been
6. Bauer, M., Cheng, S., Jain, M., Ngoy, S., Theodoropoulos, C., Trujillo, A., … Liao, R. (2011). Echocardiographic Speckle-Tracking Based Strain Imaging for Rapid Cardiovascular Phenotyping in Mice. *Circ Res2*, *108*(8), 908–916. doi:10.1161/CIRCRESAHA.110.239574.Echocardiographic
7. Bernstein, H., & Srivastava, D. (2012). Stem-cell therapy for cardiac disease. *Pediatric Research*, *71*, 491–499.
8. Bolooki, M., & Askari, A. (2011). Disease Management Project: Acute Myocardial Infarction. *Cleveland Clinic*.
9. Boudou, T., Ph, D., Legant, W. R., Mu, A., Borochin, M. A., Thavandiran, N., … Chen, C. S. (2012). A Microfabricated Platform to Measure and Manipulate the Mechanics of Engineered Cardiac Microtissues. *Tissue Engineering*, *18*, 910–919. doi:10.1089/ten.tea.2011.0341
10. Bowers, S., & Banerjee, I. (2010). The extracellular matrix: at the center of it all. *Journal of Molecular and Cellular Cardiology*, *48*(3), 474–482.
11. Chang, W.-T., Yu, D., Lai, Y.-C., Lin, K.-Y., & Liau, I. (2013). Characterization of the mechanodynamic response of cardiomyocytes with atomic force microscopy. *Analytical Chemistry*, *85*(3), 1395–400. doi:10.1021/ac3022532
12. D'Souza, M., Saaby, L., Poulsen, T. S., Diederichsen, A. C. P., Hosbond, S., Diederichsen, S. Z., … Mickley, H. (2014). Comparison of Mortality in Patients With Acute Myocardial Infarction Accidentally Admitted to Non-cardiology Departments Versus That in Patients Admitted to Coronary Care Units. *The American Journal of Cardiology*. doi:10.1016/j.amjcard.2014.07.035
13. Dunlay, S. M., Pack, Q. R., Thomas, R. J., Killian, J. M., & Roger, V. L. (2014). Participation in cardiac rehabilitation, readmissions, and death after acute myocardial infarction. *The American Journal of Medicine*, *127*(6), 538–46. doi:10.1016/j.amjmed.2014.02.008
14. Fact Sheet: International Cardiovascular Disease Statistics. (2004). *American Heart Association*.

15. Fact Sheet: The Top 10 Causes of Death. (n.d.). *World Health Organization*.
16. Franck, C., Maskarinec, S. a, Tirrell, D. a, & Ravichandran, G. (2011). Three-dimensional traction force microscopy: a new tool for quantifying cell-matrix interactions. *PloS One*, *6*(3), e17833. doi:10.1371/journal.pone.0017833
17. Guan, X., Mack, D. L., Moreno, C. M., Strande, J. L., Mathieu, J., Shi, Y., … Childers, M. K. (2014). Dystrophin-deficient cardiomyocytes derived from human urine: new biologic reagents for drug discovery. *Stem Cell Research*, *12*(2), 467–80. doi:10.1016/j.scr.2013.12.004
18. Himmel, H. M. (2013). Drug-induced functional cardiotoxicity screening in stem cell-derived human and mouse cardiomyocytes: Effects of reference compounds. *Journal of Pharmacological and Toxicological Methods*. doi:10.1016/j.vascn.2013.05.005
19. Kamakura, T., Makiyama, T., Sasaki, K., Yoshida, Y., Wuriyanghai, Y., Chen, J., … Kimura, T. (2013). Ultrastructural Maturation of Human-Induced Pluripotent Stem Cell-Derived Cardiomyocytes in a Long-Term Culture. *Circulation Journal*, *77*(5), 1307–1314. doi:10.1253/circj.CJ-12-0987
20. Kamgoué, a, Ohayon, J., Usson, Y., Riou, L., & Tracqui, P. (2009). Quantification of cardiomyocyte contraction based on image correlation analysis. *Cytometry. Part A : The Journal of the International Society for Analytical Cytology*, *75*(4), 298–308. doi:10.1002/cyto.a.20700
21. Kim, D., Kim, P., Song, I., Cha, J. M., Lee, S. H., Kim, B., & Suh, K. Y. (2006). Guided Three-Dimensional Growth of Functional Cardiomyocytes on Polyethylene Glycol Nanostructures. *Langmuir*, (22), 5419–5426.
22. Kim, D.-H., Kshitiz, Smith, R. R., Kim, P., Ahn, E. H., Kim, H.-N., … Levchenko, A. (2012). Nanopatterned cardiac cell patches promote stem cell niche formation and myocardial regeneration. *Integrative Biology : Quantitative Biosciences from Nano to Macro*, *4*(9), 1019–33. doi:10.1039/c2ib20067h
23. Kim, D.-H., Lipke, E. a, Kim, P., Cheong, R., Thompson, S., Delannoy, M., … Levchenko, A. (2010). Nanoscale cues regulate the structure and function of macroscopic cardiac tissue constructs. *Proceedings of the National Academy of Sciences of the United States of America*, *107*(2), 565–70. doi:10.1073/pnas.0906504107
24. Kim, D.-H., Wong, P. K., Park, J., Levchenko, A., & Sun, Y. (2009). Microengineered platforms for cell mechanobiology. *Annual Review of Biomedical Engineering*, *11*, 203–33. doi:10.1146/annurev-bioeng-061008-124915
25. Kim, H. N., Kang, D.-H., Kim, M. S., Jiao, A., Kim, D.-H., & Suh, K.-Y. (2012). Patterning methods for polymers in cell and tissue engineering. *Annals of Biomedical Engineering*, *40*(6), 1339–55. doi:10.1007/s10439-012-0510-y
26. Kreutziger, K., & Murry, C. (2011). Engineered Human Cardiac Tissue. *Pediatric Cardiology*, 334–341.
27. Kshitiz, Kim, D.-H., Beebe, D. J., & Levchenko, A. (2011). Micro- and nanoengineering for stem cell biology: the promise with a caution. *Trends in Biotechnology*, *29*(8), 399–408. doi:10.1016/j.tibtech.2011.03.006
28. Leong, C. M., Voorhees, A., Nackman, G. B., & Wei, T. (2013). Flow bioreactor design for quantitative measurements over endothelial cells using micro-particle image velocimetry Flow bioreactor design for quantitative measurements over endothelial cells using micro-particle image velocimetry. *Review of Scientific Instruments*, *045109*. doi:10.1063/1.4802681

29. Liau, B., Christoforou, N., Leong, K., & Bursac, N. (2011). Pluripotent Stem Cell-derived Cardiac Tissue Patch with Advanced Structure and Function. *Biomaterials*, *32*(35), 9180–9187. doi:10.1016/j.biomaterials.2011.08.050.Pluripotent
30. Lin, G., Palmer, R. E., Pister, K. S., & Roos, K. P. (2001). Miniature heart cell force transducer system implemented in MEMS technology. *IEEE Transactions on Bio-Medical Engineering*, *48*(9), 996–1006. Retrieved from http://www.ncbi.nlm.nih.gov/pubmed/11534848
31. Liu, Y., Feng, J., Shi, L., Niu, R., Sun, Q., Liu, H., … Han, D. (2012). In situ mechanical analysis of cardiomyocytes at nano scales. *Nanoscale*, *4*(1), 99–102. doi:10.1039/c1nr11303h
32. Lundy, S. D., Zhu, W.-Z., Regnier, M., & Laflamme, M. a. (2013). Structural and Functional Maturation of Cardiomyocytes Derived from Human Pluripotent Stem Cells. *Stem Cells and Development*, *22*(14). doi:10.1089/scd.2012.0490
33. Mikheev, A. M., Mikheeva, S. a, Trister, A. D., Tokita, M. J., Emerson, S. N., Parada, C. a, … Rostomily, R. C. (2014). Periostin is a novel therapeutic target that predicts and regulates glioma malignancy. *Neuro-Oncology*, (January), 1–11. doi:10.1093/neuonc/nou161
34. Milde, F., Franco, D., Ferrari, A., Kurtcuoglu, V., Poulikakos, D., & Koumoutsakos, P. (2012). Cell Image Velocimetry (CIV): boosting the automated quantification of cell migration in wound healing assays. *Integrative Biology : Quantitative Biosciences from Nano to Macro*, *4*(11), 1437–47. doi:10.1039/c2ib20113e
35. Moriguchi, H., & Madson, J. (2013). Autologous human cardiac stem cells transplantation for the treatment of ischaemic cardiomyopathy : first study of human-induced pluripotent stem (iPS) cell-derived cardiomyocytes transplantation. *BMJ Case Report*. doi:10.1136/bcr-2013-008960
36. Park, J., Kim, H., Kim, D., Levchenko, A., & Suh, K. (2012). Quantitative Analysis of the Combined Effect of Substrate Rigidity and Topographic Guidance on Cell Morphology. *IEEE Transactions on Nanobioscience*, *11*(1), 28–36.
37. Park, J., Ryu, S.-K., Kim, J., Cha, J., Baek, J., Park, S., … Lee, S. H. (2007). A three-dimensional model of fluid-structural interactions for quantifying the contractile force for cardiomyocytes on hybrid biopolymer microcantilever. *Journal of Biomechanics*, *40*(13), 2823–30. doi:10.1016/j.jbiomech.2007.03.026
38. Poveda, F., Martí, E., Gil, D., Carreras, F., & Ballester, M. (2012). Helical structure of ventricular anatomy by diffusion tensor cardiac MR tractography. *JACC. Cardiovascular Imaging*, *5*(7), 754–5. doi:10.1016/j.jcmg.2012.04.005
39. Rao, C., Prodromakis, T., & Al., E. (2013). The effect of microgrooved culture substrates on calcium cycling of cardiac myocytes derived from human induced pluripotent stem cells. *Biomaterials*, *34*(10), 2399–2411.
40. Roberts, R. G. (2001). Protein family review Dystrophins and dystrobrevins, 1–7.
41. Rodriguez, M. L., Graham, B. T., Pabon, L. M., Han, S. J., Murry, C. E., & Sniadecki, N. J. (2014). Measuring the contractile forces of human induced pluripotent stem cell-derived cardiomyocytes with arrays of microposts. *Journal of Biomechanical Engineering*, *136*(5), 051005. doi:10.1115/1.4027145
42. Saaby, L., Poulsen, T. S., Diederichsen, A. C. P., Hosbond, S., Larsen, T. B., Schmidt, H., … Mickley, H. (2014). Mortality rate in type 2 myocardial infarction: observations

from an unselected hospital cohort. *The American Journal of Medicine*, *127*(4), 295–302. doi:10.1016/j.amjmed.2013.12.020
43. Sabass, B., Gardel, M. L., Waterman, C. M., & Schwarz, U. S. (2008). High resolution traction force microscopy based on experimental and computational advances. *Biophysical Journal*, *94*(1), 207–20. doi:10.1529/biophysj.107.113670
44. Segers, V., & Lee, R. (2008). Stem cell therapy for cardiac disease. *Nature*, *451*, 937–942.
45. Sniadecki, N. J., Anguelouch, A., Yang, M. T., Lamb, C. M., Liu, Z., Kirschner, S. B., … Chen, C. S. (2007). Magnetic microposts as an approach to apply forces to living cells. *Proceedings of the National Academy of Sciences of the United States of America*, *104*(37), 14553–8. doi:10.1073/pnas.0611613104
46. Sniadecki, N. J., Lamb, C. M., Liu, Y., Chen, C. S., & Reich, D. H. (2008). Magnetic microposts for mechanical stimulation of biological cells: fabrication, characterization, and analysis. *The Review of Scientific Instruments*, *79*(4), 044302. doi:10.1063/1.2906228
47. Vunjak-Novakovic, G., Lui, K. O. ., Tandon, N., & Chien, K. R. (2011). Bioengineering Heart Muscle: A Paradigm for Regenerative Medicine. *Annual Review of Biomedical Engineering*, (13), 245–267. doi:10.1146/annurev-bioeng-071910-124701.Bioengineering
48. Xing, Y., Lv, A., Wang, L., Yan, X., Zhao, W., & Cao, F. (2012). Engineered myocardial tissues constructed in vivo using cardiomyocyte-like cells derived from bone marrow mesenchymal stem cells in rats. *Journal of Biomedical Science*, *19*(1), 6. doi:10.1186/1423-0127-19-6
49. Yu, J., Vodyanik, M., & Smuga-Otto, K. (2007). Induced pluripotent stem cell lines derived from human somatic cells. *Science*, *318*, 1917–1920.
50. Zhu, W.-Z., Biber, B., & Laflamme, M. (2011). Methods for the derivation and use of cardiomyocytes from human pluripotent stem cells. *Humana Press*.